Deleted: Submitted

The Invisible Fray: A Critical Analysis of the Use of Reflectometry for Fray Location

By Lance Griffiths****, Rohit Parakh*****,
Cynthia Furse*,**, Brittany Baker***

**Cynthia Furse corresponding author

*University of Utah
Department of Electrical and Computer Engineering
50 S Campus Drive 3280 MEB
Salt Lake City, Utah 84112
cfurse@ece.utah.edu
phone: (801) 585-7234
fax : (801) 581-5281

** LiveWire Test Labs, Inc., Salt Lake City, Utah

*** Massachusetts Institute of Technology

**** L-3 Communications, Salt Lake City, Utah

*****C-Squared Systems, Manchester, NH

Abstract
Significant international research and development efforts have been devoted to methods and equipment for locating wiring faults particularly those on aging aircraft. Several reflectometry methods that send high frequency signals down the line and analyze the returned reflections have risen to the forefront of these technologies. While these methods are proving to be accurate for location of "hard" faults (open and short circuits), location of "soft" faults such as frays and chafes remains elusive. This paper analyzes the impedance of several types of soft faults and their resultant reflectometry returns, which are shown to be smaller than returns from other sources of physical and electrical noise in the system. Through numerical simulations verified by measurement, it is shown that soft faults are virtually impossible to locate using today's reflectometry methods including time domain reflectometry, frequency domain reflectometry, and spread spectrum time domain reflectometry. The methods used in this analysis can be extended to other types of reflectometry as they emerge.

1. Introduction

Reliable wiring systems are critical to the safe operation of aircraft, power plants (nuclear and conventional), and the space shuttle. As these modern systems age, many researchers and government agencies have been working on methods to find potential faults in aging wiring [1-12]. Much of the research is based on reflectometry techniques, which send high frequency signals down the wire, and observe the reflections returned

from the junction and terminations. These methods include time domain reflectometry (TDR) [4,13] which uses a fast rise time step or pulsed signal, frequency domain reflectometry (FDR) [14] which uses multiple sinusoidal signals, sequence TDR (STDR) which uses pseudo noise, and spread spectrum TDR (SSTDR) which uses pseudo noise modulated onto a sinusoidal carrier signal for live testing with minimal interference with low frequency signals [15,24].

Location of open and short circuits is certainly a very important aspect of wire health monitoring; however there is also significant interest in locating much smaller faults before they become large enough to electrically impact the system. Chafes or frays (words generally used synonymously) occur when part of the insulation is worn away from the conductor, and perhaps even the conductor itself is damaged. This may be because of natural aging, when brittle insulation cracks and/or flakes away from the conductor. More often, frays occur when the wire rubs against the metal aircraft structure, another wire, a wire clamp, etc. Most of these faults are the results of improperly installed wire, poorly designed installations systems, or maintenance-induced damage to a previously acceptable system.

Finding the small anomalies of frayed wire before they become hard open or short circuits is of significant interest; however it is an extremely difficult problem. Chafing insulation from the conductor results in a very small change in the wire impedance. Since the reflection obtained by reflectometry depends on the impedance discontinuity, this results in a very small reflection that may be lost in the noise of the measurements. Some authors have reported success locating frays in a controlled laboratory environment. In [4], TDR is used to detect bends, heating, and compression in coaxial and unshielded wiring, in a controlled setting where the wire is not allowed to move around, is isolated from other wires, and from the physical structure of the plane.

In [9, 12] the authors observed that frays are more observable at high frequencies than low frequencies, which could potentially be used to distinguish them from the normal wire. In [21] a method for using a sliding correlator to locate the signature of the fray from within the other noise on the wire was shown to be effective even for very small faults in a highly controlled setting.

With these early analyses, there could be some hope for location of frays, however it should be noted that these tests were done in a very controlled laboratory environments. The wire is normally taped to a table or other surface to prevent movement and vibration (which create impedance changes), and carefully measured with no additional signal on the line and minimal measurement noise. The fray is then made, which generally results in a reflection too small to see in the raw data. The frayed and unfrayed signatures are subtracted, giving a response that may then show the fray. This baseline or differential approach is a natural fit for finding small changes such as frays. Unfortunately, obtaining a perfect baseline in a realistic environment is not easy. Even if you could baseline all wires on a plane, when the plane flies, the wires vibrate and move enough that the changes in the baseline may outweigh the changes due to the fray, making fray location impossible. The analysis of the reflections from the fray compared to likely changes in the baseline is the subject of this paper. This will tell us the likelihood and reliability of the fray detection capability of several reflectometry methods. In this paper TDR, FDR, and SSTDR are evaluated on small frays, large frays, water drops on the wire, and normal movement of the wires. The results do not bode

well for fray detection in general, as we shall see. Section 2 of this paper models common fray conditions using the finite difference frequency domain (FDFD) method. This gives a formal analysis of the impedance of various fray conditions. Section 3 shows results from measured frays in the lab and some ideas of measurement error associated with them. Section 4 discusses the implications of these results, and section 5 provides the conclusions from this work.

2. Simulation of Fray Impedance

The finite difference frequency domain method (FDFD) is used to calculate static voltages, fields, impedances, etc. in metallic and dielectric structures. This method is described in detail in [19] and is briefly summarized here. Laplace's equation describes the variation of voltage distribution within a system, which in this case is the cross section of a wire:

$$\nabla^2 V = \frac{\partial^2 V}{\partial x^2} + \frac{\partial^2 V}{\partial y^2} = -\frac{q}{\varepsilon} \quad (1)$$

where V is the voltage distribution, q is the charge, and ε is the permittivity, in this case of the insulating material and air surrounding the wire. This equation can be converted to its discrete difference form by dividing the cross section of the wire into a discrete grid of dimension h and applying the central difference equation to convert the derivatives to differences, yielding:

$$V(i+1, j) + V(i-1, j) + V(i, j-1) + V(i, j+1) - 4V(i, j) = -\frac{h^2 q}{\varepsilon} \quad (2)$$

where V(i,j) represents the voltage at the (i,j) location on a square grid of dimension h. This equation can be converted to a system of difference equations that can be solved for the voltage distribution by applying it at every (i,j) location within the grid. Two sets of boundary conditions are required in order to complete this solution. First, the voltage distribution on the conductors is set. One conductor is set to 1V, and the other to 0V (ground). A second boundary condition, on the outer boundary of the simulation region (outside of the wire being simulated) is set to a Dirichlet boundary sufficiently far from the wire that the voltage can be assumed to be zero. Symmetry boundary conditions can also be used to reduce the simulation region. The sparse matrix equation obtained is commonly solved for V(i,j) using an iterative method such as successive over relaxation. The electric field distribution is then found by taking the derivative (in difference form) of the voltage distribution. The capacitance per unit length can then be found from Coulomb's law by numerically integrating the electric field on any closed contour (usually a convenient rectangular region) around the positive conductor of the wire. Finally, the characteristic impedance is calculated knowing that

$$Z_0 = \frac{1}{\sqrt{LC}} \quad (3)$$

where L and C are the inductance and capacitance per unit length of the transmission line. The inductance is not known, but is the same regardless of the dielectric coating on the wire. Thus, by analyzing the transmission line with and without its dielectric insulation, the impedance can be calculated from the relative capacitance

$$Z_0 = \frac{1}{c\sqrt{CC_0}} \quad (4)$$

where c is the speed of light in a vacuum, and C_0 is the capacitance per unit length of the transmission line without any dielectric. From the impedance, the voltage reflection coefficient can be calculated (as described in section 2b). This code was written in Matlab^R .

In our simulations, one conductor of the two-wire transmission line model is set to 1V, and an outer boundary 200 cells from the transmission line is set to simulate 0V at an infinite distance. In order to model frays, a suitable two-wire conductor General Cable SKU 02301.R5.02 lamp cord shown in figure 1 is used. The wire is very similar in loss and impedance to many types of aircraft wiring, is easily and inexpensively available, and is generally used in our lab to test hardware and theory. The lamp cord consists of two wires that are surrounded by PVC insulation. The insulation is somewhat flattened as is common for this type of cable. It has the dimensions given in table 1. The wire is modeled on a 400x400 grid with 0.05 mm cells. The conductors have a radius of 0.51 mm and are separated by a distance of 2.06 mm. The insulation thickness is set to 0.76 mm, and the insulation relative permittivity is assumed to be 4.

Figure 1: General Cable SKU 02301.R5.02 lamp cord used for simulations and measurements.

Table 1: General Cable SKU 02301.R5.02 Dimensions

Cable Dimension	**(mm)**
Width	5.35
Height	2.60
wire diameter	1.00
insulation thickness on horizontal edge	1.14
insulation thickness on vertical edge	0.80
distance between inner conductor edges	1.06

a. Fray Type, Impedance, and Reflection Coefficient

The ability of a given reflectometry method to locate a fray depends on how large a reflection can be observed. This depends on the severity (impedance) of the fray, the length of the fray, and the nature of the reflectometry method. Several simulated frays were analyzed for impedances and reflection coefficients. These include:

0. Cable with no insulation (for modeling purposes only)
1. Test cable with no cuts

2. Water drop on top of insulation in center
3. Cut 0.15 mm off top of right side
4. Cut 0.45 mm off top of right side
5. Cut 0.76 mm off top of right side
6. Cut 0.15 mm off right side
7. Cut 0.45 mm off right side
8. Cut 0.76 mm off right side
9. Cut in side (cut into top on right side)
10. Water in the cut
11. Radial crack (all insulation removed on one side)
12. Water in radial crack

Figures 2 and 3 show the structure as it was modeled for each of these fray types. The voltage at each point in the simulation space was calculated using FDFD. Then the gradient was taken to compute the electric field at each point. Figure 2 shows the magnitude of the electric field of all the scenarios. Figure 3 shows the electric field direction and magnitude and the dielectric boundaries. From the capacitance calculations, (which were computed with the electric fields) the voltage reflection coefficients were calculated based on the fray type. Results of these calculations are given in table 2.

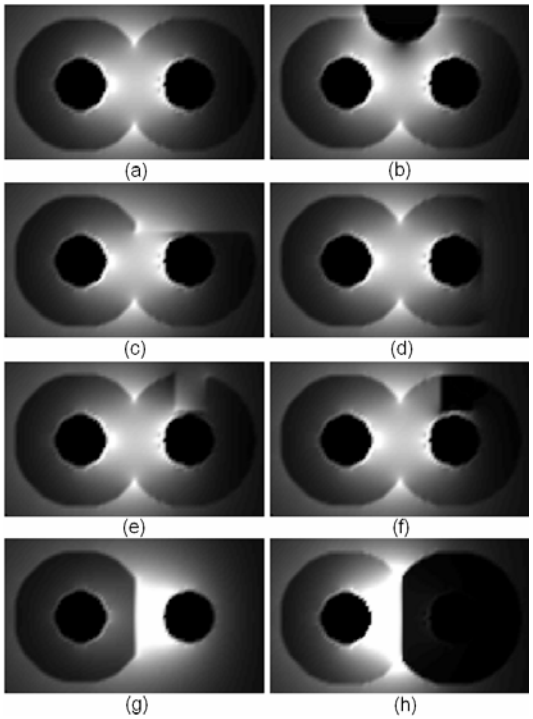

Figure 2: Electric field magnitude. Dark values are low, and white values are high. (a) Test Cable with no cuts, (b) Water Drop, (c) Cut 0.76 mm off top, (d) Cut 0.76 mm off side, (e) Groove Cut on top, (f) Water in Groove, (g) Radial Crack no insulation, (h) Water in Crack.

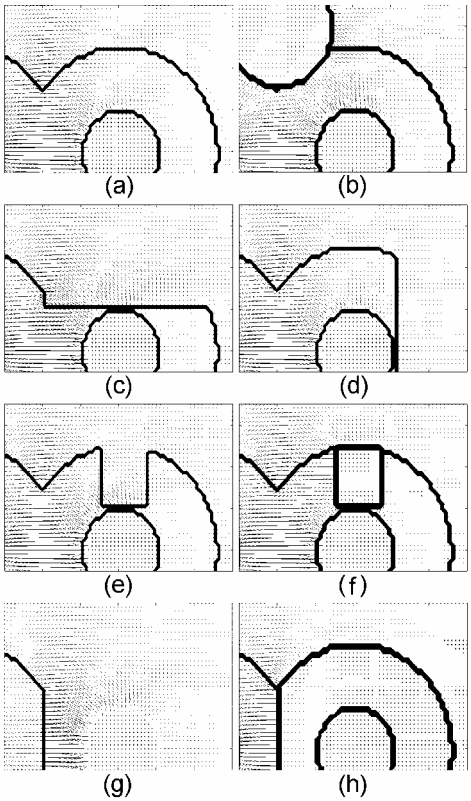

Figure 3: Lines show the magnitude and direction of the electric fields for the upper right wire. Dielectric boundaries are also shown. (a) Test Cable with no cuts, (b) Water Drop, (c) Cut 0.76 mm off top, (d) Cut 0.76 mm off side, (e) Groove Cut on top, (f) Water in Groove, (g) Radial Crack no insulation, (h) Water in Crack.

Table 2: Capacitance, characteristic impedance, and voltage reflection coefficient of simulated frays

Scenario	Label for Experiments	Capacitance F/meter	Zfray (Ω)	Voltage Reflection Coefficient (Gamma)
Open Circuit	b			1
Short Circuit	c			-1
1. Test cable with no cuts	a	6.74E-11	81.85	0
2. Water Drop		8.11E-11	74.61	-0.046277
3. Cut .15 mm off top		6.73E-11	81.9	0.000292
4. Cut .45 mm off top		6.64E-11	82.43	0.003528
5. Cut .76 mm off top	f	6.07E-11	86.26	0.026248
6. Cut .15 mm off side		6.74E-11	81.85	0.000023
7. Cut .45 mm off side		6.73E-11	81.89	0.000225
8. Cut .76 mm off side	d	6.71E-11	81.99	0.000851
9. Groove Cut on top		6.65E-11	82.38	0.00323
10. Water in Groove		6.86E-11	81.11	-0.004526
11. Radial Crack no insulation	e	2.50E-11	134.4	0.242911
12. Water in Crack		1.71E-09	16.24	-0.668869
13. ¼ conductor damage	g	3.89E-11	107.9	0.13729

The analytical solution for the characteristic impedance of a two-wire line is given by [20]

$$Z_0 = \frac{\eta_o}{\pi\sqrt{\varepsilon_r}} \cosh^{-1}\left(\frac{D}{d}\right) \tag{5}$$

where η_o is the characteristic impedance of free space (377 ohms), ε_r is the relative permittivity of the surrounding dielectric, D is the distance between the two wires (center to center), and d is the diameter of each conductor. Using the values of 2.06 mm for the center distance D between wires, a wire diameter d of 1.02 mm, and $\varepsilon_r = 4$, gives a characteristic impedance Z_0 of 79.7 ohms, which is close to the simulated value of 81.85 ohms. Variations due to finite insulation thickness account for this difference.

b. Analysis

A changing impedance on a transmission line causes a transient voltage reflection Γ, and transmission T defined by

$$\Gamma = \frac{Z_{fray} - Z_0}{Z_{fray} + Z_0} \quad (6)$$

$$T = \Gamma + 1 \quad (7)$$

where Z_{fray} is the impedance at the fray and Z_0 is the impedance of the lamp cord without any alterations. Figure 4 shows the reflections Γ and the transmissions T. At each boundary of the fray some of the signal is reflected, and the rest is transmitted. As can be seen from table 2, no significant reflections occurred unless the insulation was completely removed or water was on or in the system. The highest reflection for a fray was found when 0.76 mm was cut from the top of one of the wires giving a voltage reflection coefficient of 2.62%.

It should be noted that signals move down the wire at a speed of

$$\frac{3x10^8 m/S}{\sqrt{\varepsilon_r}} = 1.5x10^8 m/s$$

when $\varepsilon_r = 4$.

For a fray 1 cm long (which in practice would be enormous), the voltage reflection seen on a TDR due to the fray would only last

$$\frac{0.01m * 2}{1.5x10^8 m/s} = 0.133ns$$

until the secondary reflection on the other end of the fray cancels the primary reflection as shown in figure 4. Assuming infinite rise time on the TDR signal and its reflection, a 0.133 ns spike would be all that is left from the reflection at the fray. Not only is this normally immeasurable, but the rise time is also not infinite. The TDR signal is barely on its rising edge when the reflection returns to cancel it out, so in practice the "spike" is immeasurably small. In addition, the actual reflection is likely to be smaller than predicted, because the change in impedance will be continuous, rather than instantaneous.

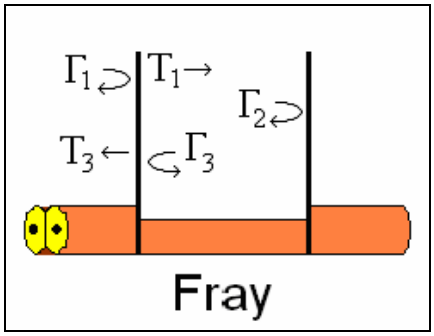

Figure 4: Reflection and transmission boundaries of a fray.

Table 3 shows the magnitude of the reflections in Figure 4 for specific simulations. The secondary reflections and transmissions quickly cancel or very nearly cancel the initial reflection, leaving only a small return, T_3. The steady state input impedance seen at a fray boundary is given by [18]

$$Z_{in}(-l) = \frac{Z_0(Z_L + Z_0 j \tan(\beta l)}{(Z_0 + Z_L j \tan(\beta l)} \qquad (8)$$

In this case the load Z_L is the characteristic impedance of the lamp cord, and Z_0 would be the impedance of the fray. β is the phase propagation coefficient and is equal to 2π / wavelength. Table 4 shows the magnitude of the reflections for various fray types vs. the percentage of fray length relative to the wavelength.

Table 3: Transient voltage reflections shown in Figure 4 for selected simulations.

Scenario/Fray Type	Γ_1	T_3
No Changes	0	0
2. Water Drop	-0.046277	-4.54E-10
5. Cut .76 mm off top	0.026248	8.55E-12
8. Cut .76 mm off side	0.000851	3.25E-22
11. Radial Crack	0.242911	4.99E-05

Table 4: The voltage reflection magnitude (T_3) is shown for a sinusoidal steady state signal, as a function of fray length.

T_3 (for Fray Length as % of Wavelength)					
Scenario/Fray Type	0.10%	1%	2%	5%	10%
No Changes	0	0	0	0	0
2. Water Drop	-3.68E-06	-3.67E-04	-1.50E-03	-8.90E-03	-0.032
5. Cut .76 mm off top	2.08E-06	2.07E-04	8.26E-04	5.00E-03	0.0181
8. Cut .76 mm off side	6.75E-08	6.74E-06	2.68E-05	1.63E-04	0.000590
11. Radial Crack	2.29E-05	2.30E-03	9.10E-03	5.29E-02	0.1747

3. Measurement Validation

In order to validate the observations with measurements, the frays given in Table 2 were created at 22 feet (6.7 meters) on a 30 foot (9.14 meters) long lamp cord. These frayed wires were then tested using TDR, FDR and SSTDR. In order to precisely control the impedance of the wire, it was laid straight and taped on a wooden table. For all methods, the response due to the frays is so small that it is very difficult or impossible to see in the raw data. Hence in all three methods a baseline response from a good wire is taken and then compared with the response of the frayed wire.

The following sections discuss the results of TDR, FDR and SSTDR. Tests are conducted on open and short circuits, insulation damaged frays and 1/4 conductor damaged frays. In the case of insulation damaged frays, the largest change in impedance occurs for the 0.76mm insulation cut from the top and side. Hence instead of including the results for all the insulation damaged frays, results for only these two cases are included.

a. Time Domain Reflectometry (TDR):

In Time Domain Reflectometry a fast rise time step or pulsed signal is transmitted on the wire. Any discontinuity on the wire (chafes, frays etc) causes a reflection which can be analyzed for information about this anomaly. A commercial TDR unit was used for these measurements. [23] The responses of the TDR for the different forms of frays described and simulated in section 2, and an open circuit (line b) and short circuit (line c) are compared with the response of a good wire (line a) and are shown in figure 5. Each line is labeled to indicate the fray type corresponding to table 2. The original good wire was 9.14 meters long, and frays or open/short circuit damage were made at 6.7 meters. The signature at the fray location is blown up for better observation in the small box on the left. Reflections other than open (b) and short (c) are so small that they are not easily seen on the original graph, but can be seen on the blown up graph. Unfortunately, it is also clear from the original graph that miscellaneous variation in the signature along the length of the line is as large as or larger than the signatures due to the frays. The signature at the end of the line is also blown up in the small box on the right. Although this is not the location where the fray should be detected, it is common to see effects from the fray at the end of the line due to the small delay the fray creates. The step function

input waveform is also seen in Figure 5, as the initial step at location 0 on the far left of figure 5.

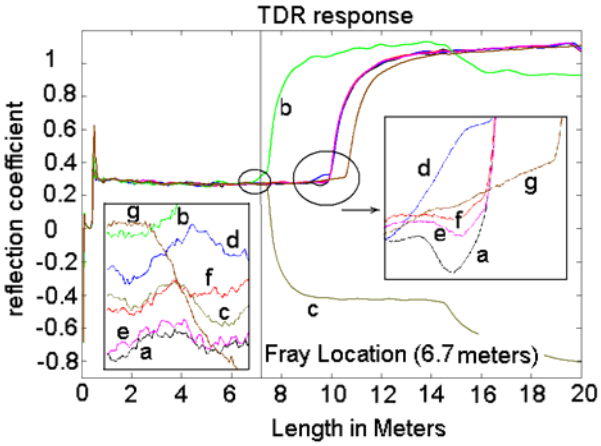

Figure 5: Response of TDR for different frays

It is difficult to visually analyze the TDR response and determine the location of the frays. The response of open and short circuits gives visibly accurate location, but for frays, the response is similar to the good wire response, and it is not possible to visibly identify the fray location. As nothing can be determined from this raw data, a sliding correlator (matched filter) is applied to augment the location of the faults as in [21]. The difference between the responses of frayed wire and the baseline (good wire response) is convolved with a predefined window function. A peak is observed in the region where the window function approximately matches the shape of the difference, which should be the response of the fray. This peak occurs only where the match is the closest, and it gives the location of any form of discontinuity. Different window functions and sizes (different matched filters) can be used for better results. The sliding correlator responses for the raw TDR data in Figure 5 are shown in Figure 6. The small signatures of the frays are blown up in the inset figure, and labeled to indicate the fray type as in table 2. Again, these signatures are too small to detect amongst the other variations on the wire, except for the open (b) and short (c). The end of the line, and the junction where the TDR is connected to the cable can also be seen. The noise level is shown, based on the peaks of the sliding correlator along the length of the cable . The sliding correlator method generally provides an improvement on the location of the fault, however it is still not sufficient to distinguish these faults from other variation on the line. For idealized test cases where the wire is taped to the table, frayed, and then retested without moving the wire 63% of the frays were identified within 0.3 m of their actual location, 13% of the frays were located within 0.3 m and 0.6 m of the prediction, and for 25% of the frays, a fray was predicted but could not be visually confirmed. These results were relatively positive, however when the wire was moved at all between tests, the faults could no longer be located, because differences in the impedance of the wire caused by moving it around produced reflections that are as significant as the reflection from the fray. All of

these differences were picked up, and the fray could not be selected from amongst all of the other differences.

It should be noted that the sliding correlator used here is an example of a matched filter used to detect small signals in noise, which has been studied extensively in the contexts of image processing, radar, sonar, echo cancellation, etc. The shape of the reflected signal can be at least approximately known based on the parameters of the wire (its transfer function) and the impedance of the fray. Thus, improved signal processing methods can improve the detection of this type of signal. Unfortunately, other types of impedance changes that are normal and expected on the wire also produce similar responses. For instance, small impedance variations caused by the wire being near a metallic structure, other wires, separation of the wire conductors (typical of uncontrolled impedance cables), etc. have as large or larger impedance variations and produce reflections that are as large or larger than the fray and of identical or very similar shape. Thus, while it is possible to create a filter that identifies the fray (such as this sliding correlator), the same filter also identifies a number of "normal" impedance variations that mask the fray, thus making it indistinguishable from the background impedance changes. The background becomes even more complex for wires in a moving vehicle that are vibrating, as the impedance changes do not remain uniform with time.

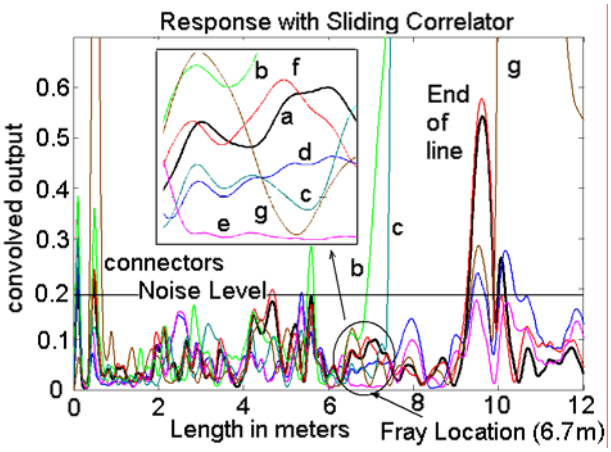

Figure 6: Response of Sliding Correlator for different frays.

It is observed that the noise due to vibrations or wire movement is an important factor in fray detection. A few peaks corresponding to frays are observed, but they are lower than the noise level. These peaks are so small that they remain hidden among peaks due to noise, which makes fault location an impossible task. Figure 7 gives a direct comparison of the peak values for different forms of discontinuities.

Deleted: Submitted

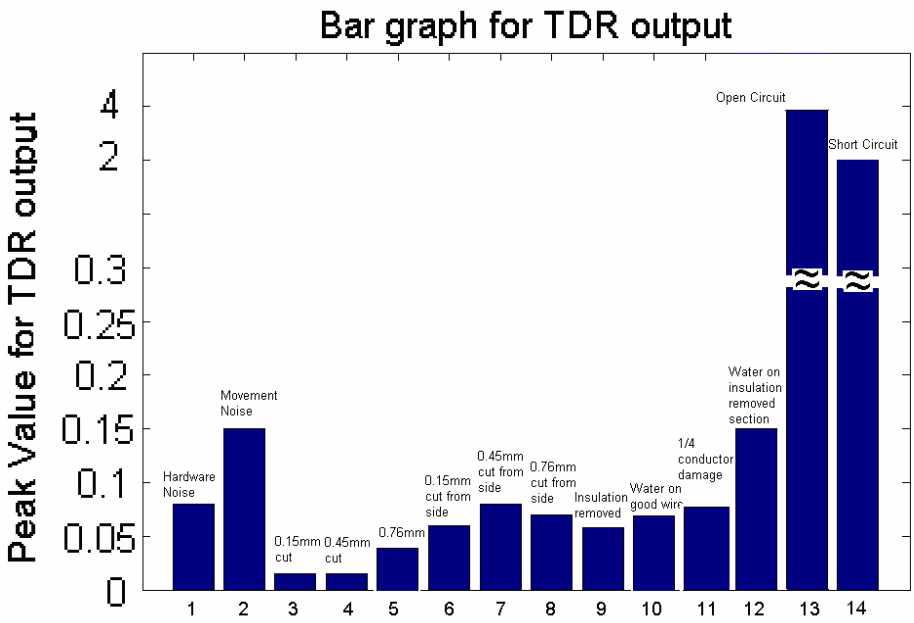

Figure 7: Peak values for different frays. (1) Hardware Noise, (2) Movement noise, (3) 0.15 mm cut from top, (4) 0.45 mm cut from top, (5) 0.76 mm cut from top, (6) 0.15 mm cut from side, (7) 0.45 mm cut from side, (8) 0.75 mm cut from side, (9) insulation removed from single side, (10) water on good wire, (11) ¼ conductor damaged, (12) water on cable with insulation removed, (13) Open Circuit, (14) Short Circuit.

It can be clearly observed in figure 7 that the peaks due to frays are similar to or less than the peaks due to noise, and hence the location of the fray cannot be determined. Only the peaks due to open or short circuits are significant and can be definitively located using TDR. From these results a conclusion can be drawn that insulation damage and, radial cracks cause a very small change in impedance which cannot be detected in a realistic environment.

The TDR data is indicative of what is seen for other reflectometry methods, as well, as will be seen in the following sections.

b. Frequency Domain Reflectometry (FDR):

Frequency Domain Reflectometry uses stepped frequency sinusoidal signals as the source signal. [14] A sinusoidal signal is transmitted on the wire, and the reflection of this wave due to a discontinuity is measured separately using a directional coupler. The incident and reflected signals are multiplied in a mixer. The mixer outputs two signals, one of which is DC and is proportional to the phase shift between to two signals. This phase shift is proportional to the electrical length of the wire, and is measured using a simple analog integrator (capacitor). The other signal is double the input frequency, and it is filtered out by the simple analog integrator, and therefore does not interfere with the

measurement. The FDR steps through a band of frequencies in this way, measuring the DC voltage that is proportional to electrical length of the wire at each frequency. This set of measurements provides a sinusoidal response, such as that seen in Figure 8. The number of cycles in this set of measurements can be found using methods such as Fourier transformation and is proportional to wire length or distance to the fault.

The hardware that was developed in house and used for these tests is described in detail in [14]. For our analysis the frequency range of the FDR is 100 MHz – 200 MHz. Figure 8 shows a typical response of a FDR for a good wire and a frayed wire.

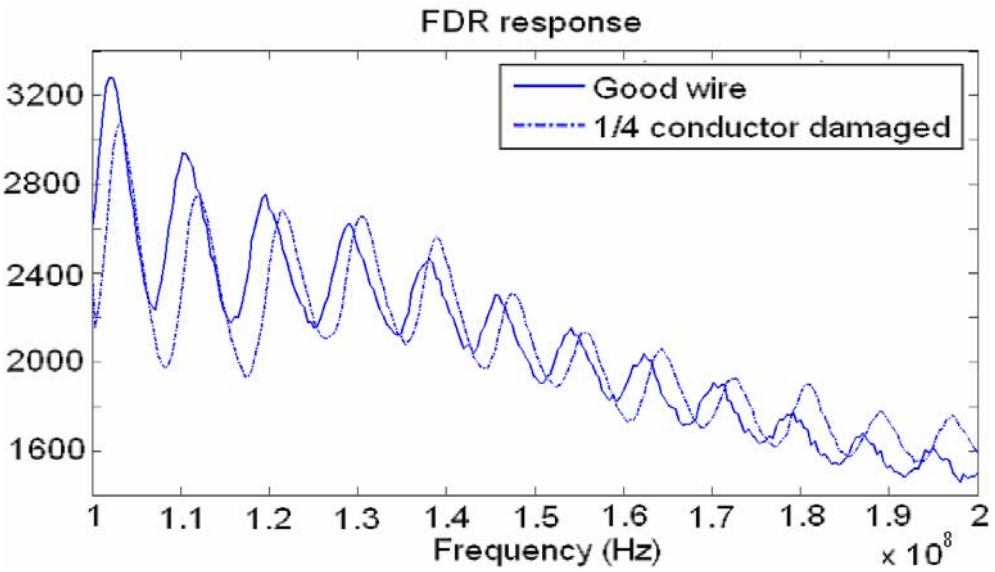

Figure 8: Typical response of FDR for good wire and frayed wire.

For further analysis, the fast Fourier transform (FFT) of the difference of these two responses is taken. This gives a peak whose location corresponds to the location of fault and whose magnitude (which is small in this case) corresponds to the magnitude of the reflection coefficient. [14] Since this peak is often too small to extract from the noise, a sliding correlator explained in the TDR section is applied, and the results are shown in Figure 9. The FDR detects open and short circuits and may detect severe conductor damage, but it cannot detect the insulation damaged and insulation removed frays.

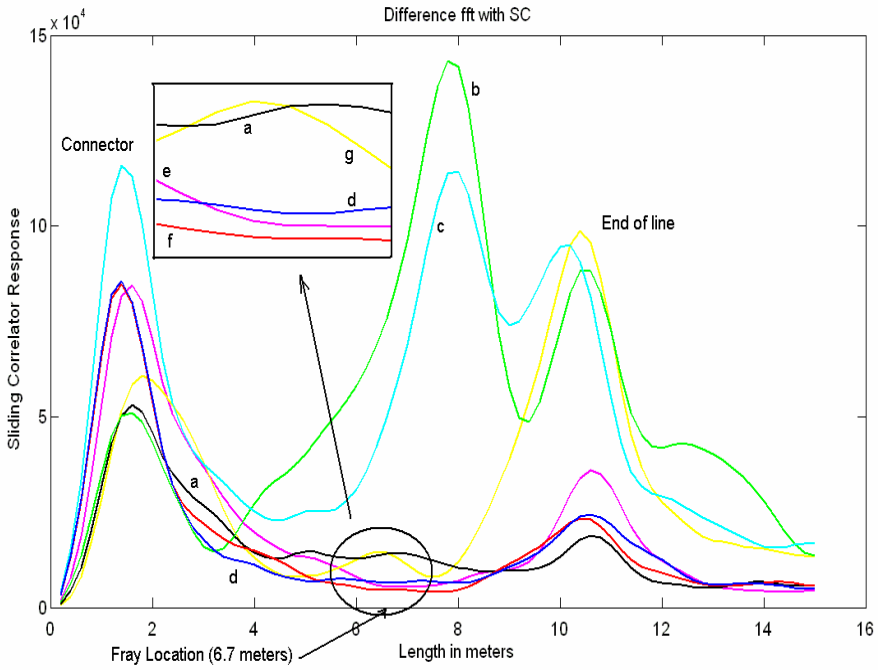

Figure 9: Sliding Correlator Response of FDR for different frays. The difference of the two signals in Figure 8 was Fourier transformed to identify locations of peaks corresponding to the reflections. A sliding correlator was applied to the transformed signals to augment the peak locations.

c. Spread Spectrum Time Domain Reflectometry (SSTDR):

Spread Spectrum Time Domain Reflectometry is used to locate faults on live wires. [15] Sequence TDR (STDR) uses a pseudo noise (PN) test signal, and spread spectrum TDR (SSTDR) uses a pseudo noise signal modulated onto a sinusoidal carrier signal for live testing without interference with existing low frequency power or higher frequency data signals [15]. The PN code for this case is 128 bits long, and has a very specific set of 1's and 0's, although to any other system, this code appears like noise. [24] The transmitted and reflected signals are correlated using hardware analog correlation, and the location of the peaks in the correlation such as those shown in Figure 10 indicate the location of the sources of reflection (faults) on the wire. Noise or existing signals on the wire are not picked up by the correlator so do not interfere with the tests. The STDR and SSTDR signals are transmitted at a level well below the 17dB noise margin of the system, so they do not interfere with the existing systems on the line. The hardware that was developed in house and used for these tests is described in detail in [15, 24]. Figure 10 shows the response of the SSTDR for different types of frays, open circuit, and short circuit compared with the response of a good wire. The STDR correlation response (not shown) has a single peak at the location of each discontinuity. The SSTDR correlation response (shown) has a triple peak at the location of each discontinuity, such as the one that can be seen at the 0 location in Figure 10. Each SSTDR peak has a large central peak with two

negative side peaks, as shown. There is always a positive peak at the 0 location where the SSTDR hardware is connected to the wire under test, because there is always an impedance discontinuity there. Later positive peaks indicate the ends of the wire (line b and the peaks due to the end of the wire at 30'). For a negative reflection coefficient, such as a short circuit, the peaks are inverted, as shown in Figure 10, line c.

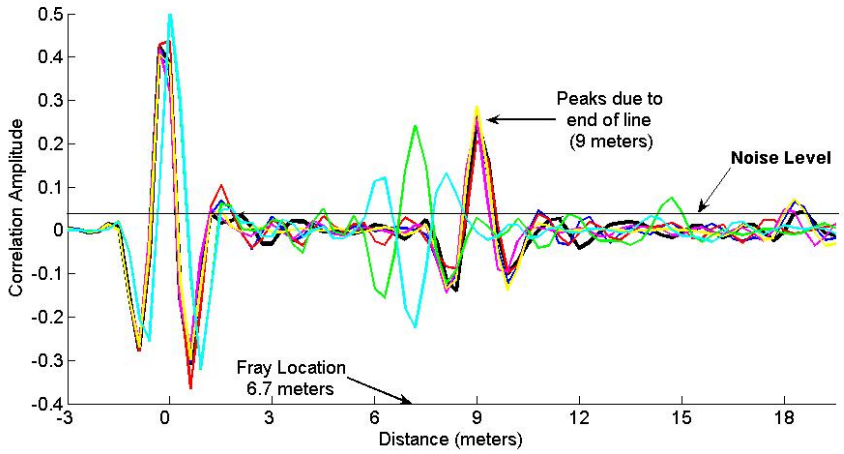

Figure 10: Response of SSTDR for different frays.

The SSTDR is able to accurately detect the open and short circuit, but it is not able to detect the other frays. The response of the frayed wire is similar to the good wire response. Its strength is for running live and detecting the intermittent open or short circuit conditions that result in chafes, frays, wet arcs, etc. It is expected that longer PN codes could reduce the noise enough to enable SSTDR to locate faults of about the same magnitude as the TDR, FDR, etc.

4. Discussion:

Over the past several years, there has been significant interest not only in finding existing faults on aging wiring, but also in being able to predict them in advance (predict them) to enable repairs during routine maintenance rather than after the system has demonstrated a fault condition. This paper analyzed the feasibility of locating small faults on wiring with reflectometry. The impedance of insulation damage, conductor damage, and water drops on the cable were calculated using the finite difference frequency domain (FDFD) method. The reflection coefficient was then calculated analytically. It was observed that the length of the fray matters significantly, because there is a reflection at both the front and back ends of the fray that approximately cancel each other out. The reflection coefficients for all but the largest conductor damage were found to be so small as to be virtually invisible. Measurements using TDR, FDR, and SSTDR were then taken, confirming these results. It was observed that simply moving the wire around in ways that could occur during regular use created more impedance changes than the fray. This means that regardless of how accurate and sensitive we make our systems, the environmental impedance changes can be expected to be larger than the

fray impedance change, making it impossible to locate the frays. Particularly problematic are moving or vibrating systems, where the background impedances change with time.

These results have some very important implications for the way we evaluate and analyze wire faults and the methods that we develop in the future to find them. First, if reflectometry cannot get a sufficient change in electrical signal to be able to locate the fault, then it is reasonable to expect that the system also is not seeing any effect from this fault. Previous inspections of aging aircraft have found literally thousands of wire faults throughout a plane, very few (hopefully none!) of which are noticeably impacting the performance of the plane at the time. If we warned the maintenance crew of every one of those faults (which we can't), this would require them to make judgments on whether or not to replace or repair wiring that has nothing wrong with it from a system point of view.

If we want to be able to prognose wiring faults, we are going to have to locate (not just detect) minute changes in system performance prior to actual symptoms of system degradation being noticed by the system. Continuous monitoring of the wires (which implies testing while the wires are live with a system such as SSTDR that does not interfere with the aircaft) could be used to local intermittent failures that predate symptomatic system performance. This seems likely to be a reasonable approach for the following reasons. First, aircraft mechanics consistently report that when a plane is brought in for routine maintenance or modification with no known problems that they will commonly find a few spots where the wire is charred or partially short circuited, implying that intermittent short circuits commonly occur without otherwise observable system degradation. The second reason we think this is feasible is that when arc fault circuit breakers are tested with wet arcs of saline dripped over two neighboring wires with radial cracks, making a water bridge, that several (often something on the order of 10-20) drips are required before the system flashes over. This would imply that similar numbers of repeated intermittent faults would occur when the wire is in the plane, as well. It is likely that most of these wet faults are too short in duration to negatively impact the performance of the system, yet they should be detectable if the wire was being continuously monitored. Thus, it is reasonable to expect that prognostics are more promising with continuous monitoring for intermittent faults than with location of frays.

The implications of continual monitoring of live wires include some sizeable advantages as well as several challenges. Methods to miniaturize SSTDR systems to enable their implementation within aircraft circuit breakers, power control systems, avionics boxes, connectors, etc. are currently under development. Conversion of existing circuit boards to integrated circuits will significantly reduce their size, cost, and power requirements. Even so, the costs in size, weight, dollars, and complexity of monitoring every wire in a legacy aircraft are probably prohibitively large. For existing planes, it may be reasonable to monitor high risk cables, cables with a history of failure, etc. It may be reasonable to include test electronics in all upgraded and repaired avionics, circuit breakers, cables, etc. And it may be reasonable to have a temporary test system that can be implemented on an "as needed" basis for diagnosis of an intermittent fault and removed once the fault has been located. New planes, particularly those currently in the design phase, may benefit the most from this type of technology, as it can be integrated

directly within the physical structure of the wiring system. Data from these sensors could be integrated directly within the existing monitoring system of the aircraft, and routine power for the sensors could be included as well. Having multiple sensors interconnected can provide many advantages including dual or multiple testing of the wiring, redundant data communication, and self-testing and diagnosing of the sensors themselves.

5. Conclusion:

This paper provides simulations and measurements (TDR, FDR, and SSTDR) for a variety of fray conditions. The most significant observation of this paper is that frays on wires have a reflectometry signature that is smaller than ordinary impedance changes on the wire and are therefore going to remain invisible to reflectometry methods. Even with further developments in the methods that might be able to make them sensitive enough to locate frays in idealized test environments, the normal impedance variation in the environment of the cable is greater than the impedance change due to the fault itself.

Acknowledgment

The authors would like to acknowledge the coding ideas and contributions from Benjamin Yang, Craig Waterman, Steven Smith, Jeff Spiegel, Darin Patch, Guillermo Oviedo Vela, Aaron Chen, Rodney Earl, Scott Adamson, and Kuncheng Zheng. This paper was initially started as a project in ECE 6340 Numerical Techniques for Electromagnetics and was expanded from there. We also wish to thank Greg Allan of CM Technologies for his very helpful discussions and TDR measurements during the preparation of this paper. This project was funded by the National Science Foundation grant # 0330465 and the Air Force Research Labs.

References:

[1] NASA, "Wiring Integrity Research (WIRE) Pilot Study A0SP-001-XB1, August 2000. available at http://wire.arc.nasa.gov/center_involvement/center.html

[2] NSTC, "Review of Federal Programs for Wire System Safety", White House Report, Nov. 2000. available at http://www.ostp.gov/html/wire_rpt.pdf

[3] C. Furse, R. Haupt, Down to the wire, IEEE Spectrum Volume: 38, no 2, Feb 2001, pp 34-39

[4] J.P. Steiner, W.L. Weeks, Time-Domain Reflectometry for Monitoring Cable Changes: Feasibility Study, EPRI GS-6642, February 1990

[5] Dana Lynch, David Wagenbach, NASA Hybrid Reflectometer: Simulation of Reflectometry in Damaged Wires, 7th Joint FAA/DoD/NASA Aging Aircraft Conference Sept. 8-11, 2003

[6] Joseph Hanson, Mathias Spies, Testing and Assessment of Electrical Systems in Aging Aircraft, 6th Joint FAA/DoD/NASA Aging Aircraft Conference Sept. 16-19, 2002

[7] Frank Hoertz, Dieter Koenig, "Studies of the early and late degradation phase of wire insulation for aircraft applications, 5th Joint NASA/FAA/DoD Conference on Aging Aircraft Sept. 10-13, 2001, Orlando, Florida

[8] Michael Dinallo, Larry Schneider, Aircraft wire systems test bed for use in development of wire-condition measurement technologies, 6th Joint FAA/DoD/NASA Aging Aircraft Conference Sept. 16-19, 2002

[9] Brent Waddoups, Cynthia Furse, Mark Schmidt, Analysis of Reflectometry for Detection of Chafed Aircraft Wiring Insulation, 5th Joint NASA/FAA/DoD Conference on Aging Aircraft Sept. 10-13, 2001, Orlando, Florida

[10] N. A. Mackay and S. R. Penstone, "High-sensitivity narrow-band time-domain reflectometer," IEEE Trans. Instrumentation and Measurement, vol. 23, no. 2, pp. 155-158, June 1974.

[11] Mark Schmidt, "Use of TDR for Cable Testing," Masters Thesis, Utah State University, 2002. (available from http://wwwlib.umi.com/dissertations/)

[12] Brent Waddoups, "Analysis of reflectometry for detection of chafed aircraft wiring insulation." Masters Thesis, Utah State University, 2001.
(available from http://wwwlib.umi.com/dissertations/)

[13] MF Iskander, Electromagnetic Fields and Waves. Englewood Cliffs, NJ: Prentice Hall, 1992.

[14] Cynthia Furse, You Chung Chung, Rakesh Dangol, Marc Nielsen, Glen Mabey, Raymond Woodward, "Frequency Domain Reflectometry for On Board Testing of Aging Aircraft Wiring," *IEEE Trans. Electromagnetic Compatibility*, Vol 45, No. 2, May 2003, *p.306-315*.

[15] C. Furse, P. Smith, M. Safavi, C. Lo, "Feasibility of Spread Spectrum Reflectometry for Location of Arcs on Live Wires," IEEE Journal of Sensors, accepted

[16] P. Tsai, Y. Chung, C. Lo, C.Furse, ,"Mixed Signal Reflectometer Hardware Implementation for Wire Fault Location," accepted to *IEEE Sensors Journal*

[17] Harry E. Green, A Simplified Derivation of the Capacitance of a Two-Wire Line, IEEE Trans on Microwave Theory and Techniques, vol. 47, no. 3, March 1999

[18] F.T. Ulaby, Fundamentals of Applied Electromagnetics, Prentice Hall, 2001

[19] Matthew N. O. Sadiku, Numerical Techniques in Electromagnetics, 2nd Ed., New York, New York: CRC Press, 2001 pp. 147-154

[20] Brian C. Wadell, Transmission Line Design Handbook, Boston: Artech House, 1991, pp. 66

[21] Alok Jani, "Location of Small Frays using TDR," Masters Thesis,Utah State University, Logan, Utah, 2003. Available from: ProQuest Information and Learning: http://wwwlib.umi.com/dissertations/

[22] Rohit Parakh, "An Invisible Fray: A formal assessment of the ability of reflectometry to locate frays on aircraft wiring", Masters Thesis, University of Utah, Salt Lake City, Utah, 2004. Available from: ProQuest Information and Learning: http://wwwlib.umi.com/dissertations/

[23] Campbell Scientific Technical Staff, *TDR100 Instruction Manual*, Campbell Scientific, ftp://ftp.campbellsci.com/pub/outgoing/manuals/tdr100.pdf.

[24] Paul Smith, "Spread Spectrum Time Domain Reflectometry," PhD Dissertation, Utah State University, Logan, Utah, 2002. Available from: ProQuest Information and Learning: http://wwwlib.umi.com/dissertations/